arXiv:1606.06648v1 [math.NA] 21 Jun 2016

A dynamical adaptive tensor method for the Vlasov-Poisson system

Virginie Ehrlacher* Damiano Lombardi†

June 22, 2016

Abstract

A numerical method is proposed to solve the full-Eulerian time-dependent Vlasov-Poisson system in high dimension. The algorithm relies on the construction of a tensor decomposition of the solution whose rank is adapted at each time step. This decomposition is obtained through the use of an efficient modified Progressive Generalized Decomposition (PGD) method, whose convergence is proved. We suggest in addition a symplectic time-discretization splitting scheme that preserves the Hamiltonian properties of the system. This scheme is naturally obtained by considering the tensor structure of the approximation. The efficiency of our approach is illustrated through time-dependent 2D-2D numerical examples.

1 Introduction

The present work investigates a numerical method for the resolution of the time-dependent Vlasov-Poisson system. The solution is approximated using parsimonious tensor methods.

In the litterature, equations arising in kinetic theory are solved by three classes of approaches: particle methods (Particle-In-Cell [22, 4, 8], Particle-In-Cloud [42]), semi-lagrangian approaches [13, 9, 29, 37, 14] and full-deterministic Eulerian methods [21, 33, 43]. In this work, we focus on the Vlasov-Poisson system as a simple yet challenging

*Université Paris Est, CERMICS, Projet Matherials, Ecole des Ponts ParisTech - INRIA, 6 & 8 avenue Blaise Pascal, 77455 Marne-la-Vallée Cedex 2, France, (ehrlachv@cermics.enpc.fr)

†INRIA Paris, (damiano.lombardi@inria.fr)

example of kinetic equation. While Eulerian approaches are appealing to describe the evolution of the unknown quantities of interest, the high dimensionality of the phase space domain make them often prohibitive in terms of memory and computational cost, especially when 2D-2D and 3D-3D problems are at hand.

The proposed method is not a particular discretization *per se*, instead, it gives a way to build a parsimonius tensor decomposition starting from chosen a priori separated discretizations for the space and the velocity variables in a full eulerian approach. The contribution is twofold: first, we show that the use of a tensorised representation of the solution induces a natural splitting of the equations which respects the Hamiltonian nature of the Vlasov-Poisson equations; second, an efficient fixed-point algorithm is proposed to solve the (non-symmetric) equations using tensorised functions. This step is performed using a modified Proper Generalized Decomposition (PGD) method [11, 20, 10, 19, 18, 5, 31], and the convergence of the scheme is proved. Let us mention that close ideas were introduced in the recent work [12] for the evolution of high-dimensional probability densities. In the contribution [29], a tensor train method is used to discretize the Vlasov-Poisson equations by separating each component, in a semi-lagrangian approach.

Here, we do not separate in all the variables in order to deal with generic space (and possibly velocity) domain geometries [43]. Thus, only second order tensors are used. The proposed method dynamically adapts through time the rank of the decomposition. This is an important feature, as was noted in [12, 29], since the number of tensorised terms needed to approximate with a given tolerance the solution at a certain time is not known *a priori*.

The structure of the work is as follows: in Section 2, the Vlasov-Poisson system is recalled in its classical and Hamiltonian formulation. A discussion on how a tensorised representation leads to a natural splitting of the evolution is presented in Section 2.3.

A second-order symplectic scheme in time is derived for the tensor representation update. Then, in Section 3, after a brief review of the PGD method for the resolution of symmetric coercive problems, a fixed-point scheme is presented, to solve some non-symmetric linear problems arising in the Vlasov-Poisson context. The proof of convergence of the algorithm is presented in Appendix A. Numerical tests illustrating the properties of the method are presented in Section 5.

2 Hamiltonian formulation and tensor decomposition

In this section, the Hamiltonian formulation of the Vlasov-Poisson system is recalled. A particular emphasis is put on the elements that play an important role in the derivation of the proposed numerical method. The idea is to compute a tensor decomposition of the solution of the Vlasov-Poisson system and to use a symplectic integrator in time in order to preserve the hamiltonian structure of the equations. As it will be shown in Section 2.3, the tensorised expansion induces a natural splitting of the equations.

2.1 The Vlasov-Poisson system

Let $d \in \mathbb{N}^*$ denote the spatial dimension of the problem and $\Omega_x, \Omega_v \subseteq \mathbb{R}^d$. The Vlasov-Poisson system for negative electric charges reads:

$$\begin{aligned} \partial_t f + v \cdot \nabla_x f - E \cdot \nabla_v f = 0, \qquad & \text{in } (0,+\infty) \times \Omega_x \times \Omega_v, \\ -\Delta_x \varphi = 1 - \int_{\Omega_v} f \, dv, \qquad & \text{in } (0,+\infty) \times \Omega_x, \\ E = -\nabla_x \varphi, \qquad & \text{in } (0,+\infty) \times \Omega_x, \\ f(0,x,v) = f_0(x,v), \qquad & \text{in } \Omega_x \times \Omega_v, \end{aligned} \tag{1}$$

with appropriate boundary conditions on $\Omega_x \times \Omega_v$, where

$$f : \left\{ \begin{array}{ccc} (0,+\infty) \times \Omega_x \times \Omega_v & \to & \mathbb{R} \\ (t,x,v) & \mapsto & f(t,x,v) \end{array} \right.$$

is the particle distribution function in the phase space, $f_0 \geq 0$ is the initial particle distribution function, $E(t,x)$ the electric fied and $\varphi(t,x)$ the electric potential. The particle density $\rho(t,x)$ is given by $\rho(t,x) = \int_{\Omega_v} f(t,x,v)\, dv$, and hence, the equation for the electric potential reads $-\Delta_x \varphi = 1 - \rho$.

The global existence of positive (weak or strong) solutions has been studied in several works [2, 3, 16, 32, 23, 28, 1].

For instance, in [32], when $\Omega_x = \Omega_v = \mathbb{R}^3$, the existence of a strong non-negative solution $f \in \mathcal{C}(\mathbb{R}_+; L^1(\mathbb{R}^3 \times \mathbb{R}^3)) \cap L^\infty(\mathbb{R}_+ \times \mathbb{R}^3 \times \mathbb{R}^3)$ is proved provided that the initial condition $f_0 \in L^1 \cap L^\infty(\mathbb{R}^3 \times \mathbb{R}^3)$ satisfies the additional condition: for some $m_0 > 3$,

$$\int_{\mathbb{R}^3 \times \mathbb{R}^3} f_0(x,v) \mid v \mid^{m_0} \, dx\, dv < +\infty.$$

For numerical purposes, equation (1) has to be solved on a truncated domain $\Omega = \Omega_x \times \Omega_v$. One can for instance impose periodic boundary conditions on $\partial\Omega_x$ or $\partial\Omega_v$, as done in [33]. An alternative formulation would consist of imposing homogeneous boundary conditions on Ω_v, the velocity domain.

Extensive reviews on the theory and numerical methods for this type of kinetic equations are detailed in [41, 15].

2.2 Hamiltonian formulation

The system (1) may be derived by using an Hamiltonian formalism (see [34]).

The Hamiltonian for the Vlasov-Poisson system reads:

$$\mathcal{H} = \int_\Omega \frac{1}{2} f \mid v \mid^2 \; dx \; dv - \int_{\Omega_x} \frac{1}{2} \varphi\rho \; dx. \tag{2}$$

The first term in the Hamiltonian is the kinetic energy of the particles, and the second term accounts for the electro-static energy. As commented in [34], the Vlasov-Poisson equations can be derived by introducing a reduced Poisson bracket:

$$\{a, b\} := \nabla_x a \cdot \nabla_v b - \nabla_v a \cdot \nabla_x b. \tag{3}$$

The evolution equation for the system can thus be written as:

$$\partial_t f = - \{f, h\}, \tag{4}$$

where $h := \frac{1}{2} \mid v \mid^2 - \varphi$ is the reduced Hamiltonian. A precise and detailed derivation of the Hamiltonian structure of the Vlasov-Poisson equations is found in [34, 35].

2.3 Splitting induced by tensor decomposition

For any measurable functions $r : \Omega_x \to \mathbb{R}$ and $s : \Omega_v \to \mathbb{R}$, we define the tensor product function $r \otimes s : \Omega_x \times \Omega_v \to \mathbb{R}$ as

$$r \otimes s : \left\{ \begin{array}{ccc} \Omega_x \times \Omega_v & \to & \mathbb{R} \\ (x, v) & \mapsto & r(x)s(v). \end{array} \right.$$

In the sequel, such a function is referred to as a *pure tensor-product* function. A linear combination of n pure tensor-product functions (for some $n \in \mathbb{N}^*$) is called a *rank-n* tensor product function.

We also introduce here the notion of tensorized operators. Let H_x (respectively H_v) be a Hilbert space of real-valued functions defined on Ω_x (respectively on Ω_v) and H a Hilbert space of functions defined on $\Omega_x \times \Omega_v$ so that $H_x \otimes H_v \subseteq H$. An operator A acting on functions depending on both x and v variables is a *tensorized operator* if it can be written as

$$A = \sum_{\lambda=1}^{L} A_x^\lambda \otimes A_v^\lambda,$$

for some $L \in \mathbb{N}^*$, where for all $1 \leq \lambda \leq L$, A_x^λ (respectively A_v^λ) is an operator on H_x (respectively on H_v). Let us remind the reader that for all operators A_x on H_x, A_v on H_v, and $(r, s) \in H_x \times H_v$,

$$(A_x \otimes A_v)(r \otimes s) = (A_x r) \otimes (A_v s).$$

In this section, a formal calculation is presented, which justifies how such a decomposition induces a natural splitting of the Vlasov-Poisson equations. Let us mention here the work [7], where a high-order splitting of the hamiltonian formulation for the Vlasov-Maxwell system was recently proposed.

In the present method, the aim is to approximate the function f, solution of (1), by a separate variate expansion of the form:

$$f(x, v, t) \approx \sum_{k=1}^{n} r_k(x, t) s_k(v, t) = \sum_{k=1}^{n} r_k(\cdot, t) \otimes s_k(\cdot, t), \tag{5}$$

with some measurable functions $r_k : \Omega_x \times \mathbb{R}_+ \to \mathbb{R}$, $s_k : \Omega_v \times \mathbb{R}_+ \to \mathbb{R}$ and $n \in \mathbb{N}^*$. When this expression is inserted into the evolution equation written in a hamiltonian form, it reads:

$$\partial_t f = -\{f, h\} \approx \sum_{k=1}^{n} -\{r_k, h\} s_k - r\{s_k, h\}. \tag{6}$$

The Poisson bracket acting on r_k and s_k, separately, can be interpreted as the operator which is inducing a dynamics on the functions r_k and s_k. Indeed, when considering $\partial_t r_k = -\{r_k, h\}$ and $\partial_t s_k = -\{s_k, h\}$, the tensor decomposition implies naturally $\partial_t f = -\{f, h\}$. Consider a particular time $t = t^*$, for which $f(x, v, t^*) \approx \sum_{k=1}^{n} r_k(x, t^*) s_k(v, t^*)$. The action of the Poisson bracket on generic functions $r(x)$ and $s(v)$ depending respectively only upon the space coordinate $x \in \Omega_x$ or the velocity $v \in \Omega_v$ reads:

$$\{r, h\} = v \cdot \nabla_x r(x), \tag{7}$$

$$\{s, h\} = \nabla_x \varphi \cdot \nabla_v s(v). \tag{8}$$

Two facts are fundamental: first, the evolution operator splits naturally into two parts, one acting on r and the other on s. Second, the evolution of each part is the action of a tensorised operator acting on the functions.

2.4 Symplectic integrator in time

Let us define $\widetilde{r}_k : (t^*, T) \times \Omega_x \times \Omega_v \to \mathbb{R}$ and $\widetilde{s}_k : (t^*, T) \times \Omega_x \times \Omega_v \to \mathbb{R}$ as solutions to the dynamical system:

$$\begin{aligned} \partial_t \widetilde{r}_k(x, v, t^*) &= -\{\widetilde{r}_k, h\}, \\ \partial_t \widetilde{s}_k(x, v, t^*) &= -\{\widetilde{s}_k, h\}, \\ \widetilde{r}_k(x, v, t^*) = r_k(x, t^*), \quad \widetilde{s}_k(x, v, t^*) &= s_k(v, t^*). \end{aligned} \tag{9}$$

At $t = t^*$, it holds that

$$\begin{aligned} \partial_t \widetilde{r}_k(x, v, t^*) &= -v \cdot \nabla_x r_k(x, t^*), \\ \partial_t \widetilde{s}_k(x, v, t^*) &= -\nabla_x \varphi(x, t^*) \cdot \nabla_v s_k(v, t^*). \end{aligned} \tag{10}$$

In other words, the time derivative of a generic element $\widetilde{r}_k$ computed at time $t = t^*$ is given by the advection part of the Vlasov-Poisson system, whereas the time derivative of the element $\widetilde{s}_k$ is given by the electrostatic force. Remark that initial functions r_k at time $t = t^*$ depend only upon x, but the time derivative depends of course also on v. The analogue is true for the s_k functions.

A symplectic discretization in time for the system (4) is proposed, based on this remark. For a comprehensive overview of geometric integrators see [27]. Let $\Delta t > 0$ be a small time step. The starting point is to consider the system (10) and use a Störmer-Verlet algorithm (see [26]) to discretize the evolution of the functions $\widetilde{r}_k$ and $\widetilde{s}_k$ between times t^* and $t^* + \Delta t$. This scheme is obtained by considering $\widetilde{r}_k$ and $\widetilde{s}_k$ as if they were the coordinates and the momenta of the Hamiltonian system associated to the Vlasov-Poisson equation. Define $\widetilde{s}_k^{(t^*)}(x, v) := \widetilde{s}_k(x, v, t^*) = s_k(v, t^*)$, $\widetilde{r}_k^{(t^*)}(x, v) := \widetilde{r}_k(x, v, t^*) = r_k(x, t^*)$, and $\widetilde{s}_k^{(t^*+\Delta t/2)}$, $\widetilde{r}_k^{(t^*+\Delta t)}$ and $\widetilde{s}_k^{(t^*+\Delta t)}$ as follows:

$$\widetilde{s}_k^{(t^*+\Delta t/2)}(x, v) = \widetilde{s}_k^{(t^*)}(x, v) + \frac{\Delta t}{2} E^{(t^*)}(x) \cdot \nabla_v \widetilde{s}_k^{(t^*+\Delta t/2)}(x, v), \tag{11}$$

$$\widetilde{r}_k^{(t^*+\Delta t)}(x, v) = \widetilde{r}_k^{(t^*)}(x, v) - \frac{\Delta t}{2} \left(v \cdot \nabla_x \widetilde{r}_k^{(t^*)}(x, v) + v \cdot \nabla_x \widetilde{s}_k^{(t^*+\Delta t/2)}(x, v) \right), \tag{12}$$

$$\widetilde{s}_k^{(t^*+\Delta t)}(x, v) = \widetilde{s}_k^{(t^*+\Delta t/2)}(x, v) + \frac{\Delta t}{2} E^{(t^*+2\Delta t/3)}(x) \cdot \nabla_v \widetilde{s}_k^{(t^*+\Delta t/2)}(x, v), \tag{13}$$

where the definitions of the electric fields are given below. Remember that $f(x,v,t^*) = \sum_{k=1}^{n} r_k(x,t)s_k(t,v)$. We define $E^{(t^*)}$ and $E^{(t^*+2\Delta t/3)}$ by

$$\begin{aligned} \rho^{(t^*)}(x) &:= \int_{\Omega_v} f(x,v,t^*)\, dv, \\ -\Delta_x \varphi^{(t^*)}(x) &= 1 - \rho^{(t^*)}(x), \\ E^{(t^*)}(x) &= -\nabla_x \varphi^{(t^*)}(x), \end{aligned} \tag{14}$$

and

$$\begin{aligned} f^{(t^*+2\Delta t/3)}(x,v) &:= \sum_{k}^{n} \widetilde{r}_k^{(t^*+\Delta t)}(x,v)\widetilde{s}_k^{(t^*+\Delta t/2)}(x,v), \\ \rho^{(t^*+2\Delta t/3)}(x) := \int_{\Omega_v} f^{(t^*+2\Delta t/3)}(x,v)\, dv &= \int_{\Omega_v} \sum_{k}^{n} \widetilde{r}_k^{(t^*+\Delta t)}\widetilde{s}_k^{(t^*+\Delta t/2)}\, dv, \\ -\Delta_x \varphi^{(t^*+2\Delta t/3)}(x) &= 1 - \rho^{(t^*+2\Delta t/3)}(x), \\ E^{(t^*+2\Delta t/3)}(x) &= -\nabla_x \varphi^{(t^*+2\Delta t/3)}(x). \end{aligned} \tag{15}$$

Defining

$$\begin{aligned} f^{(t^*)}(x,v) &:= \sum_{k}^{n} \widetilde{r}_k^{(t^*)}(x,v)\widetilde{s}_k^{(t^*)}(x,v), \\ f^{(t^*+\Delta t/3)}(x,v) &:= \sum_{k}^{n} \widetilde{r}_k^{(t^*)}(x,v)\widetilde{s}_k^{(t^*+\Delta t/2)}(x,v), \\ f^{(t^*+2\Delta t/3)}(x,v) &:= \sum_{k}^{n} \widetilde{r}_k^{(t^*+\Delta t)}(x,v)\widetilde{s}_k^{(t^*+\Delta t/2)}(x,v), \\ f^{(t^*+\Delta t)}(x,v) &:= \sum_{k}^{n} \widetilde{r}_k^{(t^*+\Delta t)}(x,v)\widetilde{s}_k^{(t^*+\Delta t)}(x,v), \end{aligned} \tag{16}$$

the above scheme can be rewritten as

$$\begin{aligned} \left(I - \frac{\Delta t}{2} E^{(t^*)} \cdot \nabla_v\right) f^{(t^*+\Delta t/3)} &= \left(I - \frac{\Delta t}{2} v \cdot \nabla_x\right) f^{(t^*)}, \\ \left(I + \frac{\Delta t}{2} v \cdot \nabla_x\right) f^{(t^*+2\Delta t/3)} &= f^{(t^*+\Delta t/3)}, \\ f^{(t^*+\Delta t)} &= \left(I + \frac{\Delta t}{2} E^{(t^*+2\Delta t/3)} \cdot \nabla_v\right) f^{(t^*+2\Delta t/3)}. \end{aligned} \tag{17}$$

This naturally leads us to define the following time-discretization scheme for the evolution of f. Set $f^{(0)} := f_0$ and for all $m \in \mathbb{N}$, define

$$\begin{aligned}\left(I - \frac{\Delta t}{2} E^{(m)} \cdot \nabla_v\right) f^{(m+1/3)} &= \left(I - \frac{\Delta t}{2} v \cdot \nabla_x\right) f^{(m)}, \\ \left(I + \frac{\Delta t}{2} v \cdot \nabla_x\right) f^{(m+2/3)} &= f^{(m+1/3)}, \\ f^{(m+1)} &= \left(I + \frac{\Delta t}{2} E^{(m+2/3)} \cdot \nabla_v\right) f^{(m+2/3)}.\end{aligned} \tag{18}$$

The function $f^{(m)}$ then gives an approximation of the solution f to (1) at time $t_m := m\Delta t$.

Of course, the starting point of the derivation of this scheme was to postulate that the function f can be written in a separate variate expansion at some time t^*. In the next section, we present the algorithm which is used at each substep of the time-discretization scheme in order to obtain a tensorized approximation of the functions $f^{(m+1/3)}$, $f^{(m+2/3)}$ and $f^{(m+1)}$ for all $m \in \mathbb{N}$, assuming that $f^{(0)}$ is given in a tensorized form.

3 Tensor methods

In this section, let H, H_x and H_v be some arbitrary Hilbert spaces so that $H_x \otimes H_v \subseteq H$. A tensor-based method is introduced to solve the following problem: find $f \in H$ solution of

$$(I + \Delta t P) f = g, \tag{19}$$

where

- g is a finite-rank tensor product element of H;
- $\Delta t \geq 0$ is a small constant;
- I is an operator on H of the form $I = I_x \otimes I_v$ where I_x (respectively I_v) is a symmetric continous coercive operator on H_x (respectively H_v);
- P is an arbitrary *tensorized* operator on H (not necessarily symmetric).

In the Vlasov-Poisson context, each step of the proposed time-discretization scheme (18) can be written under the form (19). Remark that the methodology presented hereafter

can be directly applied to other time-discretization schemes and other contexts provided that they only require the resolution of elementary subproblems of the form (19).

The approach relies on the so-called Proper Generalised Decomposition (PGD) method [30, 10, 11, 18, 36], and we first review well-known results about this method in Section 3.1. We stress on the properties of this method on an important particular case in Section 3.2. The scheme we propose is presented in Section 3.3 along with convergence results whose proofs are postponed to the appendix.

Let us highlight the philosophy of the method: the solution $f \in H$ of (19) is approximated as a sum of tensor products

$$f \approx \sum_{k=1}^{n} r_k \otimes s_k,$$

where for all $1 \leq k \leq n$, $r_k \in H_x$ and $s_k \in H_v$. Each pair (r_k, s_k) appearing in the above sum is computed in an iterative way so that the tensor product $r_k \otimes s_k$ is *the best* possible tensor product at iteration k of the algorithm. The meaning of this sentence will be made clear in the rest of the section. In the Vlasov-Poisson context, the advantage of this approach is that it only requires the resolution of linear problems for functions depending only on x or only on v. Thus, the sizes of the linear problems that are solved are much smaller than the one of the full linear problems defining the iterations of the scheme (18). We comment further on this point in Section 3.4.

3.1 PGD for coercive symmetric problems

The PGD method is related to the so-called greedy algorithms [39, 31] in nonlinear approximation theory. We review here well-known results on PGD algorithms for the approximation of high-dimensional coercive symmetric problems. We refer the reader to [19, 5, 20] for more details.

Let $\mathbf{a} : H \times H \to \mathbb{R}$ a symmetric coercive continuous bilinear form on $H \times H$ and $\mathbf{b} : H \to \mathbb{R}$ a continuous linear form on H. Let $f \in H$ the unique solution of the linear problem

$$\forall g \in H, \quad \mathbf{a}(f, g) = \mathbf{b}(g). \tag{20}$$

The existence and uniqueness of a solution f to problem (20) is a consequence of the Lax-Milgram lemma. Besides, f is equivalently the unique solution of the minimization problem

$$f \in \operatorname*{argmin}_{g \in H} \mathcal{E}(g),$$

were

$$\forall g \in H, \quad \mathcal{E}(g) := \frac{1}{2}\mathbf{a}(g,g) - \mathbf{b}(g).$$

Let us assume that the two Hilbert spaces H_x and H_v satisfy the following assumptions:

(H1) $\text{Span}\{r \otimes s,\ r \in H_x,\ s \in H_v\} \subset H$ and the inclusion is dense in H;

(H2) $\Sigma := \{r \otimes s,\ r \in H_x,\ s \in H_v\}$ is weakly closed in H.

Before presenting the PGD algorithm, we give here two simple examples of Hilbert spaces that satisfy these assumptions and are interesting in the Vlasov-Poisson context.

1. When $H = H_0^1(\Omega_x \times \Omega_v)$, the spaces $H_x = H_0^1(\Omega_x)$ and $H_v = H_0^1(\Omega_v)$ satisfy assumptions (H1)-(H2) [5].
2. In a discretized setting, when $H = \mathbb{R}^{N_x \times N_v}$ for some $N_x, N_v \in \mathbb{N}^*$, the choice $H_x = \mathbb{R}^{N_x}$ and $H_v = \mathbb{R}^{N_v}$ ensures that (H1)-(H2) holds.

Let $g_0 \in H$ be a given vector (which is usually chosen as $g_0 = 0$). The PGD algorithm to compute an approximation of f starting from the initial guess g_0 reads as follows:

PGD algorithm:

- **Initialization:** Set $n := 0$ and $f_0 := g_0$.
- **Iterate on** $n \geq 0$**:** Compute $(r_{n+1}, s_{n+1}) \in H_x \times H_v$ as a solution of the minimization problem

$$(r_{n+1}, s_{n+1}) \in \underset{(r,s) \in H_x \times H_v}{\text{argmin}} \ \mathcal{E}_n(r \otimes s), \tag{21}$$

  where for all $g \in H$, $\mathcal{E}_n(g) = \mathcal{E}(f_n + g) = \frac{1}{2}\mathbf{a}(f_n + g, f_n + g) - \mathbf{b}(f_n + g)$.
  Define $f_{n+1} := f_n + r_{n+1} \otimes s_{n+1}$ and set $n = n + 1$.

The choice of a stopping criterion is an important issue and we comment it later in this article. The method used in practice to solve (21) is detailed in Section 3.4.

The following convergence result holds:

Proposition 1. *Assume that the spaces H, H_x, H_v satisfy assumptions (H1)-(H2). Then, all the iterations of the PGD algorithm are well-defined in the sense that there exists at least one solution to problem (21) for all $n \in \mathbb{N}$. Besides, the sequence $(f_n)_{n\in\mathbb{N}}$ strongly converges in H to f.*

We refer the reader to [31, 5, 19, 20] for more details on the method and for the proof of this result. No further assumption is required at this stage on $\mathbf{a}$ or $\mathbf{b}$ for the convergence to hold. We will see in Section 3.4 that the efficiency of a PGD-based method in practice depends on the tensor decomposition of $\mathbf{a}$ and $\mathbf{b}$.

3.2 An important particular case

A remarkable situation occurs when $H = H_x \otimes H_v$ and $\mathbf{a}(\cdot,\cdot) = \langle \cdot,\cdot \rangle_H$. In this case, it holds that

$$\forall (r,s) \in H_x \times H_v, \quad \|r \otimes s\|_H = \|r\|_{H_x} \|s\|_{H_v}. \tag{22}$$

Let $\epsilon > 0$ be a small positive constant which characterizes the stopping criterion.

PGD-ϵ algorithm:

- **Initialization:** Set $n = 0$ and $f_0 = g_0$.
- **Iterate on $n \geq 0$:** Compute $(r_{n+1}, s_{n+1}) \in H_x \times H_v$ as a solution of the minimization problem

$$(r_{n+1}, s_{n+1}) \in \underset{(r,s)\in H_x\times H_v}{\operatorname{argmin}} \mathcal{E}_n(r \otimes s), \tag{23}$$

  where forall $g \in H$, $\mathcal{E}_n(g) = \frac{1}{2}\|f_n + g\|_H^2 - \mathbf{b}(g)$. Define $f_{n+1} := f_n + r_{n+1} \otimes s_{n+1}$.

  If $\|r_{n+1} \otimes s_{n+1}\|_H < \epsilon$, then stop and define $PGD(b, g_0, \epsilon) := f_{n+1}$. Otherwise, set $n = n + 1$ and iterate again.

Denoting by b the Riesz representative of the linear form $\mathbf{b}$ for the scalar product $\langle \cdot,\cdot \rangle_H$, it holds that for all $n \in \mathbb{N}^*$, (r_{n+1}, s_{n+1}) is equivalently the solution of

$$(r_{n+1}, s_{n+1}) \in \underset{(r,s)\in H_x\times H_v}{\operatorname{argmin}} \|b - f_n - r \otimes s\|_H^2. \tag{24}$$

Using the norm-product property (22), it can be proved [31] that if $g_0 = 0$, the above algorithm gives an iterative method to compute the Proper Orthogonal Decomposition

(POD) of the Riesz representative b of the linear form $\mathbf{b}$ for the scalar product $\langle \cdot, \cdot \rangle_H$. A consequence is that an approximate solution $f_n = \sum_{k=1}^{n} r_k \otimes s_k$ computed after n iterations of the PGD algorithm is a best n-rank approximation of b. In other words,

$$\|b - f_n\|_H = \min_{(\widetilde{r}_k, \widetilde{s}_k)_{1 \leq k \leq n} \in (H_x \times H_v)^n} \left\| b - \sum_{k=1}^{n} \widetilde{r}_k \otimes \widetilde{s}_k \right\|_H .$$

This optimality property is particularly interesting in the present case. In the rest of the article, we shall denote by $POD(b, \epsilon) = PGD(b, 0, \epsilon)$.

Another interesting consequence is that the sequence $(\|r_n \otimes s_n\|_H)_{n \in \mathbb{N}^*}$ of the norms of the tensor product functions given by the PGD algorithm is non-increasing. Indeed, this sequence is identical to the set of the singular values of the POD of b in $H_x \otimes H_v$ in non-increasing order [31].

Let us comment here on the use of this particular stopping criterion, which is the one we use in practice in the Vlasov-Poisson context. It holds from (23) (or equivalently (24)) that

$$\|r_{n+1} \otimes s_{n+1}\|_H = \max_{(r,s) \in H_x \times H_v} \frac{\langle b - f_n, r \otimes s \rangle_H}{\|r \otimes s\|_H}.$$

For any element $g \in H$, let us define

$$\|g\|_* := \sup_{(r,s) \ni H_x \times H_v} \frac{\langle g, r \otimes s \rangle_H}{\|r \otimes s\|_H} = \max_{(r,s) \ni H_x \times H_v} \frac{\langle g, r \otimes s \rangle_H}{\|r \otimes s\|_H}.$$

The application $g \in H \mapsto \|g\|_* \in \mathbb{R}_+$ defines a norm on H which is called the injective norm [24]. This norm is equal to the maximal singular value of the POD decomposition of g in $H_x \otimes H_v = H$. Of course, we have $\|g\|_* \leq \|g\|_H$ but these two norms are not equivalent. Thus, $\|r_{n+1} \otimes s_{n+1}\|_H$ can be seen as the injective norm of the residual of the decomposition $b - f_n$. We use the injective norm in practice as a stopping criterion because the latter quantity is much faster to evaluate than the H-norm.

3.3 Fixed-point PGD algorithm for weakly non-symmetric problems

Assume now that f is the solution of a problem of the form

$$\forall g \in H, \quad \langle f, g \rangle_H + \widetilde{\mathbf{a}}(f, g) = \mathbf{b}(g), \tag{25}$$

where $\mathbf{b}$ is a continuous linear form on H and $\widetilde{\mathbf{a}} : H \times H \to \mathbb{R}$ is a continuous bilinear form which is not symmetric nor coercive in general. There exists a unique solution of this problem for instance when $\|\widetilde{\mathbf{a}}\|_{\mathcal{L}(H\times H;\mathbb{R})} < 1$.

We still assume that we start from an initial guess for f given by an element $g_0 \in H$. A natural idea to solve (25) when $\widetilde{\mathbf{a}}$ is a *small* perturbation of the identity operator on H is to consider the following fixed-point PGD algorithm:

Fixed-point PGD algorithm:

- **Initialization:** Set $n = 0$ and $f_0 = g_0$.
- **Iterate on** $n \geq 0$**:** Compute $(r_{n+1}, s_{n+1}) \in H_x \times H_v$ as a solution of the minimization problem

$$(r_{n+1}, s_{n+1}) \in \underset{(r,s)\in H_x\times H_v}{\operatorname{argmin}} \mathcal{E}_n(r \otimes s), \tag{26}$$

  where for all $g \in H$, $\mathcal{E}_n(g) = \frac{1}{2}\langle f_n + g, f_n + g\rangle_H - \mathbf{b}(f_n + g) - \widetilde{\mathbf{a}}(f_n, f_n + g)$. Define $f_{n+1} := f_n + r_{n+1} \otimes s_{n+1}$ and set $n = n + 1$.

This algorithm was already suggested and studied in [6]. Its convergence was then proved under the condition that the Hilbert spaces H_x and H_v are finite-dimensional and that $\|\widetilde{\mathbf{a}}\|_{\mathcal{L}(H\times H)} \leq \kappa$ where κ was some constant depending on the dimension of the spaces which goes to 0 as the dimension of the spaces go to infinity. This theoretical convergence result was much more pessimistic than the numerical observations. Indeed, it was already pointed out in [6] that numerical tests indicated that this constant κ should not depend on the dimension of the spaces.

In this article, we prove that κ does not need to depend on the dimension of the Hilbert spaces, but on the number of terms appearing in the tensor decomposition of $\widetilde{\mathbf{a}}$. More precisely, let $\widetilde{A} \in \mathcal{L}(H; H)$ be the continuous linear operator on H associated to $\widetilde{\mathbf{a}}$, i.e. such that

$$\forall g_1, g_2 \in H, \quad \widetilde{\mathbf{a}}(g_1, g_2) = \langle \widetilde{A} g_1, g_2\rangle_H.$$

Then, the following result holds:

Proposition 2. *All the iterations of the Fixed-point PGD algorithm are well-defined, in the sense that for all $n \in \mathbb{N}$, there exists at least one solution to (21). Moreover, let us assume that $\widetilde{A} = \sum_{\mu=1}^{M} \widetilde{A}_x^\mu \otimes \widetilde{A}_v^\mu$ where for all $1 \leq \mu \leq M$, $\widetilde{A}_x^\mu \in \mathcal{L}(H_x; H_x)$ and*

$\widetilde{A}_v^\mu \in \mathcal{L}(H_v; H_v)$. *Let* $\kappa := \max_{1\leq\mu\leq M} \left\| \widetilde{A}_x^\mu \otimes \widetilde{A}_v^\mu \right\|_{\mathcal{L}(H;H)}$. *Assume that at least one of these two assumptions is satisfied:*

(A1) $H = H_x \otimes H_v$ *(thus the norm of* H *satisfies the norm-product property (22)) and* $3M\kappa < 1$*;*

(A2) $5M\kappa < 1$.

Then, there is a unique solution f *to (25) and the sequence* $(f_n)_{n\in\mathbb{N}}$ *strongly converges in* H *to* f.

The proof of Proposition 2 is given in the appendix. Let us point out that the convergence of the proposed algorithm is not covered in the work [25], where the authors also treat approximation of equations using tensor methods and fixed-point iterations, but with a different point of view.

In the Vlasov-Poisson context, a similar stopping criterion is used, as the one we described in Section 3.2. More precisely, for $\epsilon > 0$, $g_0 \in H$, we consider the following algorithm:

Fixed-point PGD-ϵ algorithm:

- **Initialization:** Set $n = 0$ and $f_0 = g_0$.
- **Iterate on** $n \geq 0$**:** Compute $(r_{n+1}, s_{n+1}) \in H_x \times H_v$ as a solution of the minimization problem

$$(r_{n+1}, s_{n+1}) \in \underset{(r,s)\in H_x\times H_v}{\operatorname{argmin}} \mathcal{E}_n(r \otimes s), \tag{27}$$

  where for all $g \in H$, $\mathcal{E}_n(g) = \frac{1}{2}\langle f_n + g, f_n + g\rangle_H - \mathbf{b}(f_n + g) - \widetilde{\mathbf{a}}(f_n, f_n + g)$.

  Define $f_{n+1} := f_n + r_{n+1} \otimes s_{n+1}$.

  If $\|r_{n+1} \otimes s_{n+1}\|_H < \epsilon$, then stop and define $PGD_{FP}(\widetilde{A}, b, g_0, \epsilon) := f_{n+1}$. Otherwise, set $n = n + 1$ and iterate again.

Let $b \in H$ denote the Riesz representative of $\mathbf{b}$ in H. For all $n \in \mathbb{N}$, $(r_{n+1}, s_{n+1}) \in H_x \times H_v$ is a solution to (26) if and only if it is a solution to

$$(r_{n+1}, s_{n+1}) \in \underset{(r,s)\in H_x\times H_v}{\operatorname{argmin}} \|b - (I + \widetilde{A})f_n - r \otimes s\|_H^2, \tag{28}$$

where I denotes the identity operator on H. The stopping criterion used above is justified by the fact that, for all $n \in \mathbb{N}$, $\|r_{n+1} \otimes s_{n+1}\|_H$ is equal to the injective norm of the residual of the equation $R_n := b - (I + \widetilde{A})f_n$. Indeed, (28) implies that

$$\|r_{n+1} \otimes s_{n+1}\|_H = \max_{(r,s)\in H_x \times H_v} \frac{\langle R_n, r \otimes s\rangle_H}{\|r \otimes s\|_H} = \|R_n\|_*.$$

3.4 Alternating least squares (ALS) for the practical resolution of the PGD iterations

We present in this section how minimization problems (21), (23), (26) and (27) are solved in practice. Let us point out that in all cases, at iteration $n \in \mathbb{N}$, $(r_{n+1}, s_{n+1}) \in H_x \times H_v$ is defined as a solution to

$$(r_{n+1}, s_{n+1}) \in \operatorname*{argmin}_{(r,s)\in H_x \times H_v} \mathcal{E}_n(r \otimes s), \tag{29}$$

where for all $g \in H$, $\mathcal{E}_n(g) = \frac{1}{2}\mathbf{c}(g, g) - \mathbf{l}(g)$, for some continuous linear form $\mathbf{l} : H \to \mathbb{R}$ and coercive bilinear continuous form $\mathbf{c} : H \times H \to \mathbb{R}$, wich depend on n.

Problem (29) is solved in practice using the Alternating Least Squares (ALS) [17, 40, 38] algorithm which is standard in tensor-based approximation methods. For a given error tolerance $\eta > 0$, the algorithm reads as follows:

ALS-ϵ algorithm:

- **Initialization:** Set $m = 0$ and choose randomly $r^0 \in H_x$ and $s^0 \in H_v$.
- **Iterate on** $m \geq 0$**:** Compute $r^{m+1} \in H_x$ as the unique solution of

$$r^{m+1} \in \operatorname*{argmin}_{r\in H_x} \mathcal{E}_n(r \otimes s^m). \tag{30}$$

  Then, compute $s^{m+1} \in H_v$ as the unique solution of

$$s^{m+1} \in \operatorname*{argmin}_{(s\in H_v} \mathcal{E}_n(r^{m+1} \otimes s). \tag{31}$$

  If $\|r^{m+1} \otimes s^{m+1} - r^m \otimes s^m\|_H < \eta$, set $r_{n+1} = r^{m+1}$ and $s_{n+1} = s^{m+1}$. Otherwise, set $m := m + 1$ and iterate again.

The convergence properties of this ALS algorithm are analyzed in details in [17] in the case when H_x and H_v are finite-dimensional, and for more sophisticated tensor formats. The algorithm can be shown to converge to a solution of the Euler equations associated to (29). The limit tensor product is not theoretically ensured to be the global minimum (or even a local minimum) of $(r,s) \in H_x \times H_v \mapsto \mathcal{E}_n(r \otimes s)$.

However, in practice, one can observe that it usually converges in a few iterations to a local minimum of (29). It is very commonly observed that this choice leads to very satisfactory convergence rates of PGD methods. Hence, we also use it here in the Vlasov-Poisson context.

In the rest of the article, we shall denote by $PGD(b, g_0, \epsilon, \eta)$ (respectively $PGD_{FP}(\widetilde{A}, b, g_0, \epsilon, \eta)$) the functions obtained by the PGD-ϵ (respectively Fixed-point PGD-ϵ) method when minimization problem (24) (respectively (27)) is solved using an ALS-η algorithm. We also denote by $POD(b, \epsilon, \eta) := PGD(b, 0, \epsilon, \eta)$.

We stress here on a crucial point: for the ALS algorithm to be numerically efficient in a high-dimensional context, it is important that the forms $\mathbf{c}$ and $\mathbf{l}$ admits a finite-rank tensor decomposition. Indeed, let us assume that $\mathbf{c} = \sum_{\gamma=1}^{C} \mathbf{c}_x^\gamma \otimes \mathbf{c}_v^\gamma$ and $\mathbf{l} = \sum_{\delta=1}^{D} \mathbf{l}_x^\delta \otimes \mathbf{l}_y^\delta$ for some $C, D \in \mathbb{N}^*$, such that for all $1 \leq \gamma \leq C$, $\mathbf{a}_x^\gamma \in \mathcal{L}(H_x \times H_x; \mathbb{R})$, $\mathbf{a}_v^\gamma \in \mathcal{L}(H_v \times H_v; \mathbb{R})$, and for all $1 \leq \delta \leq D$, $\mathbf{l}_x^\delta \in \mathcal{L}(H_x; \mathbb{R})$, $\mathbf{l}_v^\delta \in \mathcal{L}(H_v; \mathbb{R})$.

At each iteration $m \in \mathbb{N}^*$ of the ALS-η algorithm, $r^{m+1} \in H_x$ (respectively $s^{m+1} \in H_v$) is the unique solution to (30) (respectively (31)) if and only if it is the solution of the first-order Euler equations

$$\begin{aligned} \forall r \in H_x, \quad & \mathbf{c}(r^{m+1} \otimes s^m, r \otimes s^m) = \mathbf{l}(r \otimes s^m), \\ \forall s \in H_v, \quad & \mathbf{c}(r^{m+1} \otimes s^{m+1}, r^{m+1} \otimes s) = \mathbf{l}(r^{m+1} \otimes s). \end{aligned}$$

We clearly see that the computation of r^{m+1} and s^{m+1} only requires the resolution of a linear symmetric coercive system for functions depending only on x, or only on v. The size of the associated discretized problems are thus much smaller than those that one would have obtained to solve (25) directly for instance.

Using the tensor decomposition of $\mathbf{c}$ and $\mathbf{l}$, these equations can be rewritten as

$$\forall r \in H_x, \quad \sum_{\gamma=1}^{C} \mathbf{c}_v^\gamma(s^m, s^m)\mathbf{c}_x^\gamma(r^{m+1}, r) = \sum_{\delta=1}^{D} \mathbf{l}_v^\delta(s^m)\mathbf{l}_x^\delta(r), \tag{32}$$

$$\forall s \in H_v, \quad \sum_{\gamma=1}^{C} \mathbf{c}_v^\gamma(s^{m+1}, s)\mathbf{c}_x^\gamma(r^{m+1}, r^{m+1}) = \sum_{\delta=1}^{D} \mathbf{l}_v^\delta(s)\mathbf{l}_x^\delta(r^{m+1}). \tag{33}$$

The tensorized decomposition of $\mathbf{c}$ and $\mathbf{l}$ implies that each term appearing in (33) and (34) can be quickly evaluated, since they only involve forms defined on Hilbert spaces of functions depending on only one variable. Such tensorized decompositions are always naturally available in the Vlasov-Poisson context, and this crucial fact is at the heart of the efficiency of this approach.

4 Final algorithm for the Vlasov-Poisson system

4.1 Space and velocity discretization

Let us highlight that the proposed method can be adapted to various types of space and velocity discretizations, as well as different time schemes. It can also be adapted in other contexts than the Vlasov system. Let us assume that a discretization with N_x (respectively N_v) degrees of freedom in the x variable (respectively the v variable) is used. Thus, at each time step of the discretization scheme, the approximation of f is characterized by a matrix $f \in \mathbb{R}^{N_x \times N_v}$ which is computed in a separated form as

$$f = \sum_{k=1}^{n} r_k \otimes s_k = \sum_{k=1}^{n} r_k s_k^T,$$

with some vectors $r_k \in \mathbb{R}^{N_x \times 1}$ and $s_k \in \mathbb{R}^{N_v \times 1}$.

In this setting, the Hilbert spaces H_x, H_v and H are chosen to be $\mathbb{R}^{N_x}$, $\mathbb{R}^{N_v}$ and $\mathbb{R}^{N_x \times N_v}$. The only requirement for this strategy to be applicable is that each step of the chosen scheme requires the resolution of problems of the form (19), where P is a tensorized operator at the discrete level, and g a finite-rank element of H. More precisely, we assume that at each step of the algorithm P and g can be respectively written as

$$P = \sum_{k=1}^{p} P_x^k \otimes P_v^k \text{ and } g = \sum_{k=1}^{q} g_x^k \otimes g_v^k,$$

for some matrices $P_x^k \in \mathbb{R}^{N_x \times N_x}$, $P_v^k \in \mathbb{R}^{N_v \times N_v}$ and vectors $g_x^k \in \mathbb{R}^{N_x}$, $g_v^k \in \mathbb{R}^{N_v}$. Also, the operator I appearing in equation (19) can be written as $I = I_x \otimes I_v$ for some symmetric positive matrices $I_x \in \mathbb{R}^{N_x \times N_x}$ and $I_v \in \mathbb{R}^{N_v \times N_v}$. The space H is endowed with the scalar product

$$\forall f, g \in H, \quad \langle f, g \rangle_H := \mathrm{Tr}\left(f^T I_x g I_v\right) = \mathrm{Tr}\left(f^T (I_x \otimes I_v g)\right).$$

The idea is illustrated using a finite element discretization. Let us introduce $(\phi_i(x))_{1 \leq i \leq N_x}$ and $(\psi_k(v))_{1 \leq k \leq N_v}$ some finite element discretization bases of functions defined on Ω_x and

Ω_v respectively. Assume that these functions belong respectively to $H^1(\Omega_x)$ and $H^1(\Omega_v)$ with appropriate boundary conditions.

The following matrices are defined: for all $1 \leq \alpha \leq d$ (recall that d is the dimension of the problem), and any measurable bounded field $E = (E_\alpha)_{1\leq\alpha\leq d} : \Omega_x \to \mathbb{R}^d$,

$$\begin{aligned}
I_x &:= \left(\int_{\Omega_x} \phi_i(x)\phi_j(x)\,dx\right)_{1\leq i,j\leq N_x},\\
F_x(E_\alpha) &:= \left(\int_{\Omega_x} \phi_i(x)E_\alpha(x)\phi_j(x)\,dx\right)_{1\leq i,j\leq N_x},\\
D_{\alpha,x} &:= \left(\int_{\Omega_x} \phi_i(x)\partial_{x_\alpha}\phi_j(x)\,dx\right)_{1\leq i,j\leq N_x},\\
I_v &:= \left(\int_{\Omega_v} \psi_k(v)\psi_l(v)\,dv\right)_{1\leq k,l\leq N_v},\\
V_{\alpha,v} &:= \left(\int_{\Omega_v} \psi_k(v)v_\alpha\psi_l(v)\,dv\right)_{1\leq k,l\leq N_v},\\
D_{\alpha,v} &:= \left(\int_{\Omega_v} \psi_k(v)\partial_{v_\alpha}\psi_l(v)\,dv\right)_{1\leq k,l\leq N_v}.
\end{aligned}$$

The time scheme introduced in Section 2.4 is recalled:

$$\begin{aligned}
\left(I + \frac{\Delta t}{2}E^{(m)}\cdot\nabla_v\right) f^{(m+1/3)} &= \left(I - \frac{\Delta t}{2}v\cdot\nabla_x\right) f^{(m)},\\
\left(I + \frac{\Delta t}{2}v\cdot\nabla_x\right) f^{(m+2/3)} &= f^{(m+1/3)},\\
f^{(m+1)} &= \left(I - \frac{\Delta t}{2}E^{(m+2/3)}\cdot\nabla_v\right) f^{(m+2/3)}.
\end{aligned} \tag{34}$$

The discretized version of this scheme then reads as follows: let $f^{(0)} \in \mathbb{R}^{N_x\times N_v}$. For all $m \in \mathbb{N}$, compute $f^{(m+1/3)}, f^{(m+2/3)}, f^{(m+1)} \in \mathbb{R}^{N_x\times N_v}$ solutions of

$$\begin{aligned}
\left(I_x\otimes I_v + \frac{\Delta t}{2}\sum_{\alpha=1}^{d} F_x(E_\alpha^{(m)})\otimes D_{\alpha,v}\right) f^{(m+1/3)} &= \left(I_x\otimes I_v - \frac{\Delta t}{2}V_{\alpha,v}\otimes D_{\alpha,x}\right) f^{(m)},\\
\left(I_x\otimes I_v + \frac{\Delta t}{2}\sum_{\alpha=1}^{d} D_{\alpha,x}\otimes V_{\alpha,v}\right) f^{(m+2/3)} &= f^{(m+1/3)},\\
f^{(m+1)} &= \left(I_x\otimes I_v - \frac{\Delta t}{2}\sum_{\alpha=1}^{d} F_x(E_\alpha^{(m+2/3)})\otimes D_{\alpha,v}\right) f^{(m+2/3)}.
\end{aligned} \tag{35}$$

4.2 Summary of the algorithm in the discretized setting

The method we propose for the resolution of the Vlasov-Poisson system is summarized hereafter. Let $\epsilon > 0$ be a chosen tolerance threshold.

Verlet-PGD-ϵ algorithm:

- **Initialization:** Set $f^{(0)} = f_0$.
- **Iterate on** $m \geq 0$**:**
  - Define $P^{(m+1/3)} = \frac{\Delta t}{2} \sum_{\alpha=1}^{d} F_x(E_\alpha^{(m)}) \otimes D_{\alpha,v}$ and $g^{(m+1/3)} = \left(I_x \otimes I_v - \frac{\Delta t}{2} V_{\alpha,v} \otimes D_{\alpha,x}\right) f^{(m)}$. Compute $\overline{f}^{(m+1/3)}$ as

$$\overline{f}^{(m+1/3)} = PGD_{FP}(P^{(m+1/3)}, g^{(m+1/3)}, f^{(m)}, \epsilon, \epsilon).$$

    Recompress $\overline{f}^{(m+1/3)}$ by computing

$$f^{(m+1/3)} = POD\left(\overline{f}^{(m+1/3)}, \epsilon, \epsilon\right).$$

  - Define $P^{(m+2/3)} = \frac{\Delta t}{2} \sum_{\alpha=1}^{d} D_{\alpha,x} \otimes V_{\alpha,v}$. Compute $\overline{f}^{(m+2/3)}$ as

$$\overline{f}^{(m+2/3)} = PGD_{FP}(P^{(m+1/3)}, f^{(m+1/3)}, f^{(m+1/3)}, \epsilon, \epsilon).$$

    Recompress $\overline{f}^{(m+2/3)}$ by computing

$$f^{(m+2/3)} = POD\left(\overline{f}^{(m+2/3)}, \epsilon, \epsilon\right).$$

  - Define $Q^{(m+1)} = -\frac{\Delta t}{2} \sum_{\alpha=1}^{d} F_x(E_\alpha^{(m+2/3)}) \otimes D_{\alpha,v}$. Compute $f^{(m+1)}$ as

$$f^{(m+1)} = POD((I_x \otimes I_v + Q^{(m+1)}) f^{(m+2/3)}, \epsilon, \epsilon).$$

The condition we obtained in Proposition 2 on the convergence of the Fixed-point PGD algorithm implies that the time step $\Delta t > 0$ has to be taken sufficiently small to ensure that the norms of the operators entering in the decomposition of $P^{m+1/3}$ and $P^{m+2/3}$ are also small. In practice, we thus observe that our scheme suffers from a type of CFL condition that has to be respected for the method to converge. Apart from this

restriction which does not appear to be too penalizing in practice, the approach proposed here is very flexible and yields promising numerical results as shown in the next section.

5 Numerical results

In this section some numerical experiments are presented, to assess the properties of the method. First, two 1D-1D examples are considered, to validate the proposed approach. The following quantities are monitored: the error in mass, momentum and energy conservation, and the error with respect to a reference solution. The L_2 averaged in time relative errors are defined as follows:

$$\epsilon_m := \frac{1}{M\, t_f} \left(\int_0^{t_f} (m - m(0))^2 \; dt \right)^{1/2}, \tag{36}$$

$$\epsilon_p := \frac{1}{P\, t_f} \left(\int_0^{t_f} (p - p(0))^2 \; dt \right)^{1/2}, \tag{37}$$

$$\epsilon_h := \frac{1}{H(0)\, t_f} \left(\int_0^{t_f} (h - h(0))^2) \; dt \right)^{1/2}, \tag{38}$$

$$\epsilon_f := \frac{1}{t_f} \left(\int_0^{t_f} \frac{\int_\Omega (f_{ref} - f)^2 \; dx \; dv}{\int_\Omega f_{ref}^2 \; dx \; dv} \; dt \right)^{1/2}, \tag{39}$$

where t_f is the final time of the simulation, M is the normalising mass factor, defined as the mass of the initial condition $M = m(0) = \int_\Omega f_0 \; dx \; dv$, $P = \sqrt{2MK}$ is the momentum reference value, where $K = \int_\Omega f_0 \frac{v^2}{2} \; dx \; dv$ is the initial kinetic energy, and $H(0)$ is the Hamiltonian at initial time.

In the last part of this section, a 2D-2D example is shown to illustrate the applicability of the method in more high-dimensional settings. Simulations on 3D-3D testcases is work in progress.

5.1 Landau Damping.

The first test proposed is a standard linear Landau damping in a 1D-1D configuration, as proposed in [33]. The domain size is $\Omega_x = [0, 4\pi]$ and $\Omega_v = [-10, 10]$. Periodic (respectively homogeneous Dirichlet) boundary conditions are set on Ω_x (respectively

Ω_v). The initial condition is given in analytical form as:

$$f(x, v; t = 0) = F(x)G(v), \tag{40}$$

$$F(x) = 1 + \beta \cos(kx), \tag{41}$$

$$G(v) = \frac{1}{\sqrt{2\pi}} \exp\left(-\frac{v^2}{2}\right), \tag{42}$$

where $k = 0.5$ is the wavenumber of the perturbation and the amplitude $\beta = 0.01$ set the problem in a linear Landau damping regime (see [33, 29]). In such a configuration the analytical decay rate for the electric amplitude is $\gamma \approx 0.153$. For this test a mixed discretization is set up: for the space, a spectral collocation method is used based on a Fourier discretization, whereas for the velocity standard centered finite differences are used.

The numerical experiments are done by varying the space and velocity resolution, the time step, and the tolerance on the residual. For the space and the velocity discretization, we take $N_x = N_v = (32, 64, 128, 256)$. The final time is set to $t_f = 10.0$ and the number of iterations is $N_t = (4 \cdot 10^3, 8 \cdot 10^3, 16 \cdot 10^3)$. The tolerance on the residual is chosen as $\varepsilon = (10^{-10}, 10^{-12}, 10^{-14}, 10^{-16})$. For the reference simulation $N_x = N_v = 512$, $N_t = 32 \cdot 10^3$ and $\varepsilon = 10^{-18}$.

The results of the numerical testcases are reported in Table 1. The numerical experiments show that the conservation of mass, momentum and hamiltonian are well respected for all the discretizations adopted. Concerning the error with respect to the reference simulation, it has been observed that the error is dominated by the space-time discretization. In particular, using a residual tolerance (ε) too low with a given discretization does not allow to improve the results. On the other hand, when refining the mesh or when using a small Δt, a high tolerance may result in a non-convergence of the solution. In Figure 1 the decay in electrostatic energy is shown as a function of time for $N_x = N_v = (32, 64, 128)$, compared to the theoretical decay. The behavior in terms of decay and of Langmuir frequency is in agreement with the results presented in the litterature.

Let us mention here that the memory needed to store a rank-n function is $n(N_x+N_v)$, which has to be compared with N_xN_v, the total number of degrees of freedom in the system. The evolution in time of the ranks of the approximation of f computed by the approach is plotted in Figure 2 for the following discretization parameters: $N_x = N_v = 512$, $\epsilon = 10^{-16}$, $N_t = 32000$, and $T = 10$. We observe that the maximal rank of the approximation is obtained at the final time of the simulation and is approximately equal to $n = 50$. The worst compression factor $\frac{N_xN_v}{n(N_x+N_v)} \approx 5$ remains reasonable in this 1d

Table 1: Errors in the conserved quantities and with respect to a reference simulation for the 1D-1D Landau Damping testcase (section 5.1)

resolution (N_x – N_t – ε)	ϵ_m	ϵ_p	ϵ_h	ϵ_f
$32 - 4 \cdot 10^3 - 10^{-10}$	$9.09 \cdot 10^{-7}$	$5.18 \cdot 10^{-6}$	$8.52 \cdot 10^{-5}$	$1.06 \cdot 10^{-3}$
$32 - 4 \cdot 10^3 - 10^{-12}$	$1.12 \cdot 10^{-6}$	$6.24 \cdot 10^{-6}$	$2.43 \cdot 10^{-5}$	$4.15 \cdot 10^{-4}$
$32 - 4 \cdot 10^3 - 10^{-14}$	$1.02 \cdot 10^{-7}$	$5.59 \cdot 10^{-6}$	$1.01 \cdot 10^{-5}$	$4.14 \cdot 10^{-4}$
$32 - 4 \cdot 10^3 - 10^{-16}$	$7.08 \cdot 10^{-8}$	$5.60 \cdot 10^{-6}$	$9.45 \cdot 10^{-6}$	$4.14 \cdot 10^{-4}$
$32 - 8 \cdot 10^3 - 10^{-10}$	$3.64 \cdot 10^{-6}$	$6.90 \cdot 10^{-6}$	$9.31 \cdot 10^{-4}$	$3.28 \cdot 10^{-3}$
$32 - 8 \cdot 10^3 - 10^{-12}$	$1.11 \cdot 10^{-6}$	$6.28 \cdot 10^{-6}$	$2.48 \cdot 10^{-5}$	$4.05 \cdot 10^{-4}$
$32 - 8 \cdot 10^3 - 10^{-14}$	$4.32 \cdot 10^{-7}$	$5.60 \cdot 10^{-6}$	$1.60 \cdot 10^{-5}$	$4.05 \cdot 10^{-4}$
$32 - 8 \cdot 10^3 - 10^{-16}$	$6.71 \cdot 10^{-8}$	$5.64 \cdot 10^{-6}$	$8.75 \cdot 10^{-6}$	$4.05 \cdot 10^{-4}$
$32 - 16 \cdot 10^3 - 10^{-10}$	$4.38 \cdot 10^{-6}$	$7.57 \cdot 10^{-6}$	$1.04 \cdot 10^{-3}$	$3.40 \cdot 10^{-3}$
$32 - 16 \cdot 10^3 - 10^{-12}$	$1.04 \cdot 10^{-6}$	$6.31 \cdot 10^{-6}$	$2.32 \cdot 10^{-5}$	$4.01 \cdot 10^{-4}$
$32 - 16 \cdot 10^3 - 10^{-14}$	$1.14 \cdot 10^{-6}$	$6.31 \cdot 10^{-6}$	$2.46 \cdot 10^{-5}$	$4.01 \cdot 10^{-4}$
$32 - 16 \cdot 10^3 - 10^{-16}$	$6.01 \cdot 10^{-8}$	$5.67 \cdot 10^{-6}$	$8.53 \cdot 10^{-6}$	$4.00 \cdot 10^{-4}$
$64 - 4 \cdot 10^3 - 10^{-10}$	$6.75 \cdot 10^{-7}$	$2.61 \cdot 10^{-6}$	$8.33 \cdot 10^{-5}$	$9.71 \cdot 10^{-4}$
$64 - 4 \cdot 10^3 - 10^{-12}$	$8.58 \cdot 10^{-7}$	$3.19 \cdot 10^{-6}$	$1.98 \cdot 10^{-5}$	$1.33 \cdot 10^{-4}$
$64 - 4 \cdot 10^3 - 10^{-14}$	$2.11 \cdot 10^{-7}$	$2.68 \cdot 10^{-6}$	$1.08 \cdot 10^{-5}$	$1.28 \cdot 10^{-4}$
$64 - 4 \cdot 10^3 - 10^{-16}$	$1.54 \cdot 10^{-8}$	$2.68 \cdot 10^{-6}$	$8.32 \cdot 10^{-6}$	$1.28 \cdot 10^{-4}$
$64 - 8 \cdot 10^3 - 10^{-10}$	$1.21 \cdot 10^{-6}$	$2.70 \cdot 10^{-6}$	$3.29 \cdot 10^{-4}$	$2.91 \cdot 10^{-3}$
$64 - 8 \cdot 10^3 - 10^{-12}$	$8.70 \cdot 10^{-7}$	$3.19 \cdot 10^{-6}$	$1.92 \cdot 10^{-5}$	$1.30 \cdot 10^{-4}$
$64 - 8 \cdot 10^3 - 10^{-14}$	$8.64 \cdot 10^{-7}$	$2.61 \cdot 10^{-6}$	$2.14 \cdot 10^{-5}$	$1.28 \cdot 10^{-4}$
$64 - 8 \cdot 10^3 - 10^{-16}$	$1.77 \cdot 10^{-8}$	$2.69 \cdot 10^{-6}$	$8.38 \cdot 10^{-6}$	$1.25 \cdot 10^{-4}$
$64 - 16 \cdot 10^3 - 10^{-10}$	$1.42 \cdot 10^{-6}$	$3.61 \cdot 10^{-6}$	$2.62 \cdot 10^{-4}$	$3.30 \cdot 10^{-3}$
$64 - 16 \cdot 10^3 - 10^{-12}$	$9.95 \cdot 10^{-7}$	$3.19 \cdot 10^{-6}$	$2.15 \cdot 10^{-5}$	$1.28 \cdot 10^{-4}$
$64 - 16 \cdot 10^3 - 10^{-14}$	$9.25 \cdot 10^{-7}$	$3.19 \cdot 10^{-6}$	$2.03 \cdot 10^{-5}$	$1.28 \cdot 10^{-4}$
$64 - 16 \cdot 10^3 - 10^{-16}$	$3.10 \cdot 10^{-8}$	$2.71 \cdot 10^{-6}$	$8.54 \cdot 10^{-6}$	$1.23 \cdot 10^{-4}$

resolution (N_x – N_t – ε)	ϵ_m	ϵ_p	ϵ_h	ϵ_f
$128 - 4 \cdot 10^3 - 10^{-10}$	$4.45 \cdot 10^{-7}$	$1.29 \cdot 10^{-6}$	$9.31 \cdot 10^{-5}$	$1.13 \cdot 10^{-3}$
$128 - 4 \cdot 10^3 - 10^{-12}$	$1.07 \cdot 10^{-6}$	$1.69 \cdot 10^{-6}$	$1.97 \cdot 10^{-5}$	$7.60 \cdot 10^{-5}$
$128 - 4 \cdot 10^3 - 10^{-14}$	$2.49 \cdot 10^{-7}$	$1.34 \cdot 10^{-6}$	$1.10 \cdot 10^{-5}$	$6.30 \cdot 10^{-5}$
$128 - 4 \cdot 10^3 - 10^{-16}$	$1.44 \cdot 10^{-8}$	$1.33 \cdot 10^{-6}$	$8.45 \cdot 10^{-6}$	$6.26 \cdot 10^{-5}$
$128 - 8 \cdot 10^3 - 10^{-10}$	$9.93 \cdot 10^{-7}$	$1.45 \cdot 10^{-6}$	$1.73 \cdot 10^{-4}$	$2.87 \cdot 10^{-3}$
$128 - 8 \cdot 10^3 - 10^{-12}$	$1.18 \cdot 10^{-6}$	$1.71 \cdot 10^{-6}$	$2.20 \cdot 10^{-5}$	$6.92 \cdot 10^{-5}$
$128 - 8 \cdot 10^3 - 10^{-14}$	$8.40 \cdot 10^{-7}$	$1.38 \cdot 10^{-6}$	$1.96 \cdot 10^{-5}$	$6.48 \cdot 10^{-5}$
$128 - 8 \cdot 10^3 - 10^{-16}$	$2.31 \cdot 10^{-8}$	$1.34 \cdot 10^{-6}$	$8.60 \cdot 10^{-6}$	$6.07 \cdot 10^{-5}$
$128 - 16 \cdot 10^3 - 10^{-10}$	$8.75 \cdot 10^{-7}$	$1.71 \cdot 10^{-6}$	$3.90 \cdot 10^{-4}$	$3.29 \cdot 10^{-3}$
$128 - 16 \cdot 10^3 - 10^{-12}$	$1.45 \cdot 10^{-6}$	$1.67 \cdot 10^{-6}$	$2.56 \cdot 10^{-5}$	$6.79 \cdot 10^{-5}$
$128 - 16 \cdot 10^3 - 10^{-14}$	$1.10 \cdot 10^{-6}$	$1.69 \cdot 10^{-6}$	$2.14 \cdot 10^{-5}$	$6.79 \cdot 10^{-5}$
$128 - 16 \cdot 10^3 - 10^{-16}$	$4.13 \cdot 10^{-8}$	$1.35 \cdot 10^{-6}$	$8.79 \cdot 10^{-6}$	$5.98 \cdot 10^{-5}$
$256 - 4 \cdot 10^3 - 10^{-10}$	*n.c.*	*n.c.*	*n.c.*	*n.c.*
$256 - 4 \cdot 10^3 - 10^{-12}$	$1.03 \cdot 10^{-6}$	$7.69 \cdot 10^{-7}$	$1.99 \cdot 10^{-5}$	$8.88 \cdot 10^{-5}$
$256 - 4 \cdot 10^3 - 10^{-14}$	$2.54 \cdot 10^{-7}$	$6.68 \cdot 10^{-7}$	$1.13 \cdot 10^{-5}$	$5.73 \cdot 10^{-5}$
$256 - 4 \cdot 10^3 - 10^{-16}$	$2.54 \cdot 10^{-7}$	$6.68 \cdot 10^{-7}$	$1.12 \cdot 10^{-5}$	$5.73 \cdot 10^{-5}$
$256 - 8 \cdot 10^3 - 10^{-10}$	$9.28 \cdot 10^{-7}$	$6.99 \cdot 10^{-7}$	$1.61 \cdot 10^{-4}$	$2.87 \cdot 10^{-3}$
$256 - 8 \cdot 10^3 - 10^{-12}$	$9.77 \cdot 10^{-7}$	$8.14 \cdot 10^{-7}$	$1.93 \cdot 10^{-5}$	$9.01 \cdot 10^{-5}$
$256 - 8 \cdot 10^3 - 10^{-14}$	$8.35 \cdot 10^{-7}$	$6.99 \cdot 10^{-7}$	$1.93 \cdot 10^{-5}$	$5.94 \cdot 10^{-5}$
$256 - 8 \cdot 10^3 - 10^{-16}$	$1.55 \cdot 10^{-8}$	$6.72 \cdot 10^{-7}$	$8.52 \cdot 10^{-6}$	$5.49 \cdot 10^{-5}$
$256 - 16 \cdot 10^3 - 10^{-10}$	$5.02 \cdot 10^{-7}$	$7.87 \cdot 10^{-7}$	$6.46 \cdot 10^{-4}$	$3.32 \cdot 10^{-3}$
$256 - 16 \cdot 10^3 - 10^{-12}$	$1.64 \cdot 10^{-6}$	$8.14 \cdot 10^{-7}$	$2.73 \cdot 10^{-5}$	$6.83 \cdot 10^{-5}$
$256 - 16 \cdot 10^3 - 10^{-14}$	$1.37 \cdot 10^{-6}$	$7.68 \cdot 10^{-7}$	$2.35 \cdot 10^{-5}$	$6.24 \cdot 10^{-5}$
$256 - 16 \cdot 10^3 - 10^{-16}$	$3.04 \cdot 10^{-8}$	$6.75 \cdot 10^{-7}$	$8.69 \cdot 10^{-6}$	$5.41 \cdot 10^{-5}$

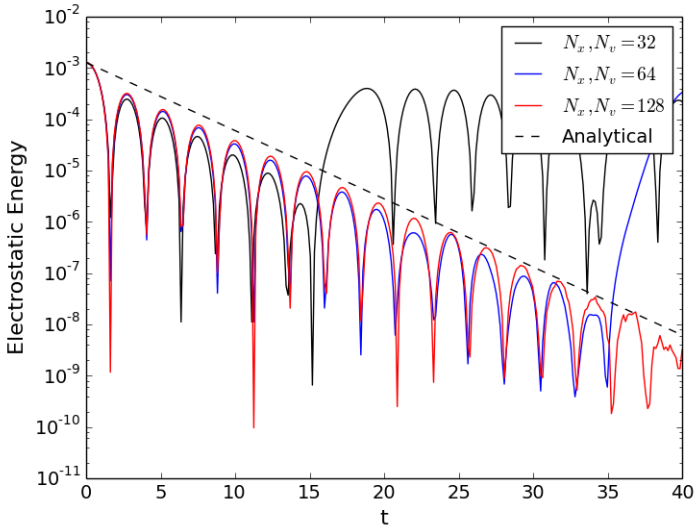

Figure 1: Linear Landau damping testcase (see section 5.1). Electrostatic energy as function of time for different resolutions in the phase space. Dash line is the analytical expected decay for the electrostatic energy.

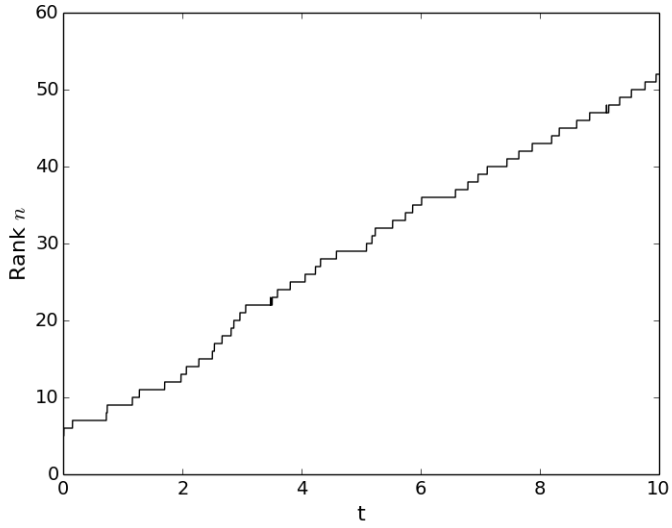

Figure 2: Evolution in time of the rank of the approximation of f.

case. We observe numerically an interesting trend: the rank seems to increase linearly with time and are independent of N_x and N_v.

5.2 Two stream instability.

We present the classical 1D-1D two stream-instability testcase. The domain is $\Omega = \Omega_x \times \Omega_v = [0, 10\pi/\omega] \times [-10, 10]$.

The final time of the evolution is $T = 36.0$. The initial condition has the following form:

$$f(x, v; t = 0) = F(x)G(v), \tag{43}$$

$$F(x) = 1 + \beta \cos(kx), \tag{44}$$

$$G(v) = \frac{1}{\sqrt{4\pi}} \exp\left(-\frac{(v - v_0)^2}{2}\right) + \frac{1}{\sqrt{4\pi}} \exp\left(-\frac{(v + v_0)^2}{2}\right), \tag{45}$$

where $v_0 = 2.4$ and $\beta = 10^{-3}$. A mixed discretization is considered, namely a spectral collocation method for the space and standard centered finite differences in velocity. The contour plot of the reference solution at final time is shown in Figure 3. The conservation properties and the errors with respect to a reference simulation are investigated by

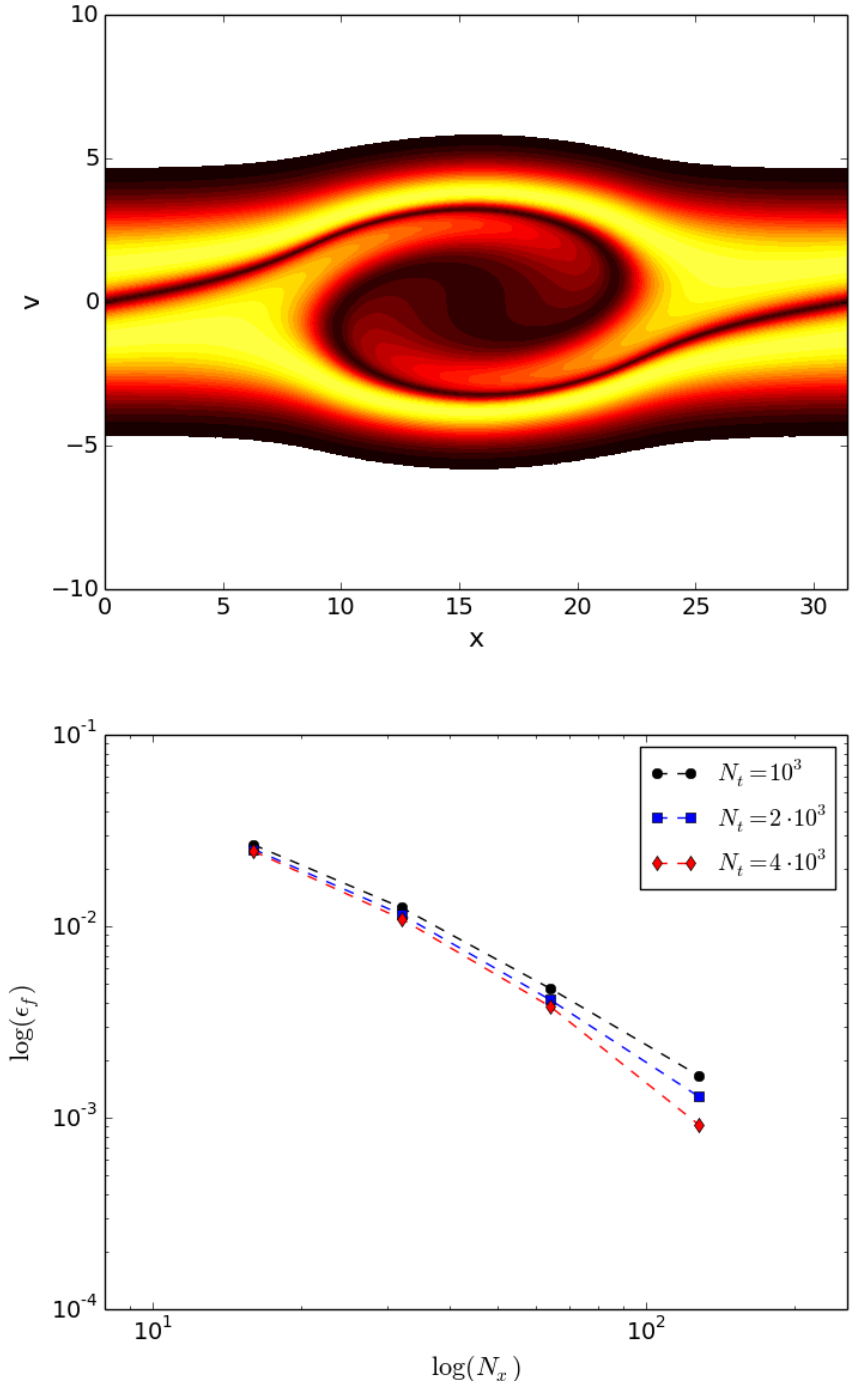

Figure 3: Two stream instability testcase (section 5.2): a) Contours of the reference solution (black for the lowest value) at final time and b) Errors with respect to a reference simulation as function of the phase space discretization, for different time steps.

varying the phase space discretization as well as time step and the residual tolerance. The results are very similar to the ones obtained for the linear Landau damping testcase. For the sake of brevity, the conservation error properties are not reported. The errors with respect to a reference simulation ($N_x = 256,\ N_v = 512,\ N_t = 8 \cdot 10^3, \varepsilon = 10^{-14}$) are computed by varying the discretization of the phase space and the time step. In particular, N_x ranges in $[16, 32, 64, 128]$, $N_v = 2N_x$ and $N_t = [10^3, 2 \cdot 10^3, 4 \cdot 10^3]$. The tolerance on the residual is varied and the errors when considering $\varepsilon = 10^{-12}$ are shown in Figure 3. A second order convergence rate is retrieved for the space discretization, at fixed time step. Whereas the error is relatively insensitive to the time step when a coarse discretization is considered, a definite dependence is seen for the finest grid resolution. This is due to the fact that, on the coarse grids, the discretization error is dominated by the space discretization error.

5.3 2D-2D simulations

In this section, we present a 2D-2D Landau damping test case. The simulation domains are $\Omega_x = (0, 4\pi)^2$ and $\Omega_v = (-10, 10)^2$. We impose as before periodic boundary conditions on Ω_x and homogeneous Dirichlet boundary conditions on Ω_v. Uniform tensor discretizations are used for Ω_x and Ω_v, and two different simulations are obtained for the following numbers of degrees of freedom: $(N_x, N_v) = [(16^2, 32^2), (32^2, 64^2)]$. The error tolerance criterion of the algorithm is set to be $\epsilon = 10^{-15}$. Time step is equal to $\Delta t = 2.10^{-4}$.

The initial condition is defined as

$$f_0(x, v) = \frac{1}{\sqrt{2\pi}^3} \left[1 - \beta \sin(\omega x_1) - \beta \sin(\omega x_2)\right] \exp(-\frac{1}{2}(v_1^2 + v_2^2)),$$

where $\beta = 0.01$ and $\omega = 0.5$.

The evolution of the electric energy as a function of time is shown in Figure 4 for the two different discretizations mentioned above. It can be seen that these are in agreement with the predicted analytical decay. Conservation properties of mass, momentum and total energy behave similarly to 1D-1D cases. Ranks of the approximated solution obtained by the algorithm also seem to increase linearly with time.

We mention here that encouraging preliminary results have been obtained on 3D-3D test cases. Parallelisation of the method, which is needed to reduce the computational cost, is work in progress, and should enable to obtain results in more realistic settings.

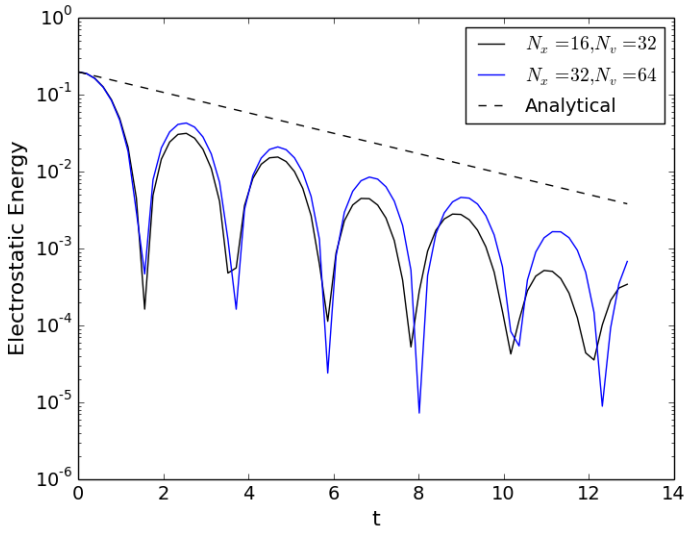

Figure 4: Evolution of the electric energy as a function of time in the 2D Landau damping test case.

6 Conclusion

In this work a dynamical adaptive tensor method has been proposed to build parsimonious discretizations for the Vlasov-Poisson system. It allows to treat generic geometries and can be applied to generic heterogeneous discretizations in space and velocity, making it a flexible tool for the simulation of kinetic equation within an Eulerian framework. The method is dynamical in time and the time advancing is design to preserve the Hamiltonian character of the system, with a second order accuracy. Several testcases were proposed to validate the method and assess its properties.

Several perspectives arise, concerning the parallelisation of the method (which is mandatory to deal with more realistic 3D-3D settings) and its extension to other kinetic equations, involving collision operators. These will be the object of a further investigation.

Appendix A: Proof of Proposition 2

Proof of Proposition 2. Let us denote by $b \in H$ the Riesz representative of $\mathbf{b}$ in H. The element f solution of (25) is then the unique solution to

$$(I + \widetilde{A})f = b,$$

where I denotes the identity operator on H. By assumption, $\|\widetilde{A}\|_{\mathcal{L}(H;H)} \leq M\kappa$, thus both (A1) or (A2) imply that $\|\widetilde{\mathbf{a}}\|_{\mathcal{L}(H\times H;\mathbb{R})} < 1$. For all $n \in \mathbb{N}$, let us denote by $R_n := b - (I + \widetilde{A})f_n$ the residual of the equation in H after n iterations of the Fixed-point PGD algorithm. Since $(r_{n+1}, s_{n+1}) \in H_x \times H_v$ is solution to the minimization problem (26), it satisfies

$$(r_{n+1}, s_{n+1}) \in \underset{(r,s)\in H_x\times H_v}{\operatorname{argmin}} \|R_n - r \otimes s\|_H^2. \tag{46}$$

Thus, we have the following properties on the tensor product function $r_{n+1} \otimes s_{n+1}$

$$(r_{n+1}, s_{n+1}) \in \operatorname{argmax}_{(r,s)\in H_x\times H_v} \tfrac{\langle R_n, r\otimes s\rangle_H}{\|r\otimes s\|_H}, \tag{47}$$

$$\|r_{n+1} \otimes s_{n+1}\|_H = \max_{(r,s)\in H_x\times H_v} \tfrac{\langle R_n, r\otimes s\rangle_H}{\|r\otimes s\|_H}, \tag{48}$$

$$\langle R_n - r_{n+1} \otimes s_{n+1}, r_{n+1} \otimes s_{n+1}\rangle_H = 0.$$

We refer the reader to [31, 5, 18, 19, 20] for a proof of the properties (47), (48) and (49), which are consequences of (46). Let us already point out here that if $H = H_x \otimes H_v$ (which is the case when assumption (A1) is satisfied), we have in addition

$$\max_{(r,s)\in H_x\times H_v} \frac{\langle R_n - r_{n+1} \otimes s_{n+1}, r \otimes s\rangle_H}{\|r \otimes s\|_H} \leq \|r_{n+1} \otimes s_{n+1}\|_H. \tag{49}$$

Thus, since $f_{n+1} = f_n + r_{n+1} \otimes s_{n+1}$,

$$\begin{aligned}
\|R_n\|_H^2 - \|R_{n+1}\|_H^2 &= \|R_n\|_H^2 - \|R_n - r_{n+1} \otimes s_{n+1} - \widetilde{A} r_{n+1} \otimes s_{n+1}\|_H^2, \\
&= \|R_n\|_H^2 - \|R_n - r_{n+1} \otimes s_{n+1}\|^2 - \|\widetilde{A} r_{n+1} \otimes s_{n+1}\|_H^2 \\
&\quad + 2\langle R_n - r_{n+1} \otimes s_{n+1}, \widetilde{A} r_{n+1} \otimes s_{n+1} \rangle_H, \\
&= \|R_n\|_H^2 - \|R_n\|_H^2 + \|r_{n+1} \otimes s_{n+1}\|_H^2 - \|\widetilde{A} r_{n+1} \otimes s_{n+1}\|_H^2 \\
&\quad + 2\langle R_n - r_{n+1} \otimes s_{n+1}, \widetilde{A} r_{n+1} \otimes s_{n+1} \rangle_H, \qquad \text{(using (49))} \\
&= + \|r_{n+1} \otimes s_{n+1}\|_H^2 - \|\widetilde{A} r_{n+1} \otimes s_{n+1}\|_H^2 \\
&\quad + 2 \sum_{\mu=1}^{M} \langle R_n - r_{n+1} \otimes s_{n+1}, (A_x^\mu r_{n+1}) \otimes (A_v^\mu s_{n+1}) \rangle_H, \\
&\geq (1 - \kappa M) \|r_{n+1} \otimes s_{n+1}\|_H^2 + 2 \sum_{\mu=1}^{M} \langle R_n - r_{n+1} \otimes s_{n+1}, (A_x^\mu r_{n+1}) \otimes (A_v^\mu s_{n+1}) \rangle_H.
\end{aligned}$$

At this point, we treat the two cases separately. Let us first assume that (A1) holds. Then,

$$\begin{aligned}
\|R_n\|_H^2 - \|R_{n+1}\|_H^2 &\geq (1 - \kappa M) \|r_{n+1} \otimes s_{n+1}\|_H^2 \\
&\quad - 2 \sum_{\mu=1}^{M} \|r_{n+1} \otimes s_{n+1}\|_H \|(A_x^\mu r_{n+1}) \otimes (A_v^\mu s_{n+1})\|_H, \qquad \text{(using (49))} \\
&= (1 - \kappa M) \|r_{n+1} \otimes s_{n+1}\|_H^2 \\
&\quad - 2 \sum_{\mu=1}^{M} \|r_{n+1} \otimes s_{n+1}\|_H \|(A_x^\mu \otimes A_v^\mu)(r_{n+1} \otimes s_{n+1})\|_H, \\
&\geq (1 - \kappa M) \|r_{n+1} \otimes s_{n+1}\|_H^2 - 2 \sum_{\mu=1}^{M} \kappa \|r_{n+1} \otimes s_{n+1}\|_H^2, \\
&\geq (1 - 3\kappa M) \|r_{n+1} \otimes s_{n+1}\|_H^2.
\end{aligned}$$

Assume now that (A2) holds. Then,

$$\begin{aligned}
\|R_n\|_H^2 - \|R_{n+1}\|_H^2 &\geq (1-\kappa M)\|r_{n+1}\otimes s_{n+1}\|_H^2 \\
&\quad -4\sum_{\mu=1}^{M}\|r_{n+1}\otimes s_{n+1}\|_H\|(A_x^\mu r_{n+1})\otimes(A_v^\mu s_{n+1})\|_H, \quad \text{(using (48))} \\
&= (1-\kappa M)\|r_{n+1}\otimes s_{n+1}\|_H^2 - 4\sum_{\mu=1}^{M}\|r_{n+1}\otimes s_{n+1}\|_H\|(A_x^\mu\otimes A_v^\mu)(r_{n+1}\otimes s_{n+1})\|_H, \\
&\geq (1-\kappa M)\|r_{n+1}\otimes s_{n+1}\|_H^2 - 4\sum_{\mu=1}^{M}\kappa\|r_{n+1}\otimes s_{n+1}\|_H^2, \\
&\geq (1-5\kappa M)\|r_{n+1}\otimes s_{n+1}\|_H^2.
\end{aligned}$$

In both cases, there exists a constant $\eta > 0$ such that

$$\|R_n\|_H^2 - \|R_{n+1}\|_H^2 \geq \eta\|r_{n+1}\otimes s_{n+1}\|_H^2.$$

Thus, the sequence $(\|R_n\|_H^2)_{n\in\mathbb{N}}$ is non-increasing and converges. Since $\|\widetilde{A}\|_{\mathcal{L}(H;H)} < 1$, and $R_n = b - (\widetilde{A}+I)f_n$, this implies that $(f_n)_{n\in\mathbb{N}}$ is a bounded sequence in H. Besides, the series $\sum_{n\in\mathbb{N}^*}\|r_n\otimes s_n\|_H^2$ is convergent, and $\|r_n\otimes s_n\|_H \underset{n\to+\infty}{\longrightarrow} 0$. Up to the extraction of a subsequence (still denoted $(f_n)_{n\in\mathbb{N}}$ for the sake of simplicity), $(f_n)_{n\in\mathbb{N}}$ weakly converges in H to some $g \in H$. Property (48) implies that

$$\forall (r,s)\in H_x\times H_v, \quad |\,\langle R_n, r\otimes s\rangle_H\,| = |\,\langle b-(I+\widetilde{A})f_n, r\otimes s\rangle_H\,| \leq \|r_{n+1}\otimes s_{n+1}\|_H\|r\otimes s\|_H.$$

Since $b-(I+\widetilde{A})f_n \underset{n\to+\infty}{\rightharpoonup} b-(I+\widetilde{A})g$, we obtain that g is necessarily equal to f, the unique solution of (25). The sequence $(f_n)_{n\in\mathbb{N}}$ thus entirely converges (weakly) to f in H. The strong convergence can be obtained using the same arguments as in [5], which yields the desired result. □

References

[1] Luigi Ambrosio, Maria Colombo, and Alessio Figalli. On the lagrangian structure of transport equations: the Vlasov-Poisson system. *arXiv preprint arXiv:1412.3608*, 2014.

[2] Aleksei Alekseevich Arsenev. Existence in the large of a weak solution to the Vlasov system of equations. *Zhurnal Vychislitelnoi Matematiki i Matematicheskoi Fiziki*, 15:136–147, 1975.

[3] Claude Bardos and Pierre Degond. Global existence for the Vlasov-Poisson equation in 3 space variables with small initial data. In *Annales de l'IHP Analyse non linéaire*, volume 2, pages 101–118, 1985.

[4] JU Brackbill. On energy and momentum conservation in particle-in-cell plasma simulation. *Journal of Computational Physics*, 317:405–427, 2016.

[5] Eric Cances, Virginie Ehrlacher, and Tony Lelievre. Convergence of a greedy algorithm for high-dimensional convex nonlinear problems. *Mathematical Models and Methods in Applied Sciences*, 21(12):2433–2467, 2011.

[6] Eric Cances, Virginie Ehrlacher, and Tony Lelievre. Greedy algorithms for high-dimensional non-symmetric linear problems. In *ESAIM: Proceedings*, volume 41, pages 95–131. EDP Sciences, 2013.

[7] Fernando Casas, Nicolas Crouseilles, Erwan Faou, and Michel Mehrenberger. High-order hamiltonian splitting for Vlasov-Poisson equations. *arXiv preprint arXiv:1510.01841*, 2015.

[8] Paul Cazeaux and Jan S Hesthaven. Multiscale time-integration for particle-in-cell methods. Technical report, Elsevier, 2014.

[9] Frédérique Charles, Bruno Després, and Michel Mehrenberger. Enhanced convergence estimates for semi-lagrangian schemes application to the Vlasov–Poisson equation. *SIAM Journal on Numerical Analysis*, 51(2):840–863, 2013.

[10] Francisco Chinesta, Amine Ammar, and Elías Cueto. Recent advances and new challenges in the use of the proper generalized decomposition for solving multidimensional models. *Archives of Computational methods in Engineering*, 17(4):327–350, 2010.

[11] Francisco Chinesta, Pierre Ladeveze, and Elías Cueto. A short review on model order reduction based on proper generalized decomposition. *Archives of Computational Methods in Engineering*, 18(4):395–404, 2011.

[12] H Cho, D Venturi, and GE Karniadakis. Numerical methods for high-dimensional probability density function equations. *Journal of Computational Physics*, 305:817–837, 2016.

[13] Nicolas Crouseilles, Guillaume Latu, and Eric Sonnendrücker. A parallel Vlasov solver based on local cubic spline interpolation on patches. *Journal of Computational Physics*, 228(5):1429–1446, 2009.

[14] Nicolas Crouseilles, Michel Mehrenberger, and Eric Sonnendrücker. Conservative semi-lagrangian schemes for Vlasov equations. *Journal of Computational Physics*, 229(6):1927–1953, 2010.

[15] Pierre Degond, Lorenzo Pareschi, and Giovanni Russo. *Modeling and computational methods for kinetic equations*. Springer Science & Business Media, 2004.

[16] Laurent Desvillettes and Jean Dolbeault. On long time asymptotics of the VlasovPoissonBoltzmann equation. *Communications in partial differential equations*, 16(2-3):451–489, 1991.

[17] Mike Espig and Aram Khachatryan. Convergence of alternating least squares optimisation for rank-one approximation to high order tensors. *arXiv preprint arXiv:1503.05431*, 2015.

[18] Antonio Falco and Anthony Nouy. A proper generalized decomposition for the solution of elliptic problems in abstract form by using a functional eckart–young approach. *Journal of Mathematical Analysis and Applications*, 376(2):469–480, 2011.

[19] Antonio Falcó and Anthony Nouy. Proper generalized decomposition for nonlinear convex problems in tensor banach spaces. *Numerische Mathematik*, 121(3):503–530, 2012.

[20] Leonardo E Figueroa and Endre Süli. Greedy approximation of high-dimensional Ornstein–Uhlenbeck operators. *Foundations of Computational Mathematics*, 12(5):573–623, 2012.

[21] Francis Filbet and Eric Sonnendrücker. Comparison of eulerian vlasov solvers. *Computer Physics Communications*, 150(3):247–266, 2003.

[22] Kai Germaschewski, William Fox, Stephen Abbott, Narges Ahmadi, Kristofor Maynard, Liang Wang, Hartmut Ruhl, and Amitava Bhattacharjee. The plasma simulation code: A modern particle-in-cell code with patch-based load-balancing. *Journal of Computational Physics*, 318:305–326, 2016.

[23] Robert T Glassey. *The Cauchy problem in kinetic theory*. SIAM, 1996.

[24] Alexandre Grothendieck. Résumé de la théorie métrique des produits tensoriels topologiques. *Resenhas do Instituto de Matemática e Estatística da Universidade de São Paulo*, 2(4):401–481, 1996.

[25] Wolfgang Hackbusch, Boris N Khoromskij, and Eugene E Tyrtyshnikov. Approximate iterations for structured matrices. *Numerische Mathematik*, 109(3):365–383, 2008.

[26] Ernst Hairer, Christian Lubich, and Gerhard Wanner. Geometric numerical integration illustrated by the Störmer–Verlet method. *Acta numerica*, 12:399–450, 2003.

[27] Ernst Hairer, Christian Lubich, and Gerhard Wanner. *Geometric numerical integration: structure-preserving algorithms for ordinary differential equations*, volume 31. Springer Science & Business Media, 2006.

[28] Hyung Ju Hwang. Regularity for the Vlasov–Poisson system in a convex domain. *SIAM journal on mathematical analysis*, 36(1):121–171, 2004.

[29] Katharina Kormann. A semi-lagrangian Vlasov solver in tensor train format. *SIAM Journal on Scientific Computing*, 37(4):B613–B632, 2015.

[30] Pierre Ladeveze, J-C Passieux, and David Néron. The latin multiscale computational method and the proper generalized decomposition. *Computer Methods in Applied Mechanics and Engineering*, 199(21):1287–1296, 2010.

[31] Claude Le Bris, Tony Lelievre, and Yvon Maday. Results and questions on a nonlinear approximation approach for solving high-dimensional partial differential equations. *Constructive Approximation*, 30(3):621–651, 2009.

[32] PIERRE-LOUIS Lions and BENOIT Perthame. Propagation of moments and regularity for the 3-dimensional Vlasov-Poisson system. *Inventiones mathematicae*, 105(1):415–430, 1991.

[33] Éric Madaule, Marco Restelli, and Eric Sonnendrücker. Energy conserving discontinuous Galerkin spectral element method for the Vlasov–Poisson system. *Journal of Computational Physics*, 279:261–288, 2014.

[34] Jerrold E. Marsden and Alan Weinstein. The hamiltonian structure of the Maxwell-Vlasov equations. *Physica D: Nonlinear Phenomena*, 4(3):394 – 406, 1982.

[35] PJ Morrison. Hamiltonian and action principle formulations of plasma physicsa). *Physics of Plasmas (1994-present)*, 12(5):058102, 2005.

[36] Anthony Nouy. A priori model reduction through proper generalized decomposition for solving time-dependent partial differential equations. *Computer Methods in Applied Mechanics and Engineering*, 199(23):1603–1626, 2010.

[37] Martin Campos Pinto and Michel Mehrenberger. Convergence of an adaptive semi-lagrangian scheme for the Vlasov-Poisson system. *Numerische Mathematik*, 108(3):407–444, 2008.

[38] Thorsten Rohwedder and André Uschmajew. On local convergence of alternating schemes for optimization of convex problems in the tensor train format. *SIAM Journal on Numerical Analysis*, 51(2):1134–1162, 2013.

[39] Vladimir N Temlyakov. Greedy approximation. *Acta Numerica*, 17:235–409, 2008.

[40] André Uschmajew. Local convergence of the alternating least squares algorithm for canonical tensor approximation. *SIAM Journal on Matrix Analysis and Applications*, 33(2):639–652, 2012.

[41] Victor Vedenyapin, Alexander Sinitsyn, and Eugene Dulov. *Kinetic Boltzmann, Vlasov and Related Equations*. Elsevier, 2011.

[42] Xingyu Wang, Roman Samulyak, Xiangmin Jiao, and Kwangmin Yu. AP-Cloud: Adaptive Particle-in-Cloud method for optimal solutions to Vlasov–Poisson equation. *Journal of Computational Physics*, 316:682–699, 2016.

[43] Jin Xu, Peter N Ostroumov, Brahim Mustapha, and Jerry Nolen. Scalable direct vlasov solver with discontinuous galerkin method on unstructured mesh. *SIAM Journal on Scientific Computing*, 32(6):3476–3494, 2010.